

## Molecular Inclusion in Functionalized Macrocycles. Part 8.<sup>1</sup> The Crystal and Molecular Structure of Calix[4]arene from Phenol and its (1:1) and (3:1) Acetone Clathrates

Rocco Ungaro\* and Andrea Pochini

*Istituto di Chimica Organica dell'Università di Parma, Via M. D'Azeglio 85, 43100 Parma, Italy*

Giovanni D. Andreotti\* and Vincenzo Sangermano

*Istituto di Strutturistica Chimica dell'Università and Centro di Studio per la Strutturistica Diffraattometrica del CNR, Via M. D'Azeglio 85, 43100 Parma, Italy*

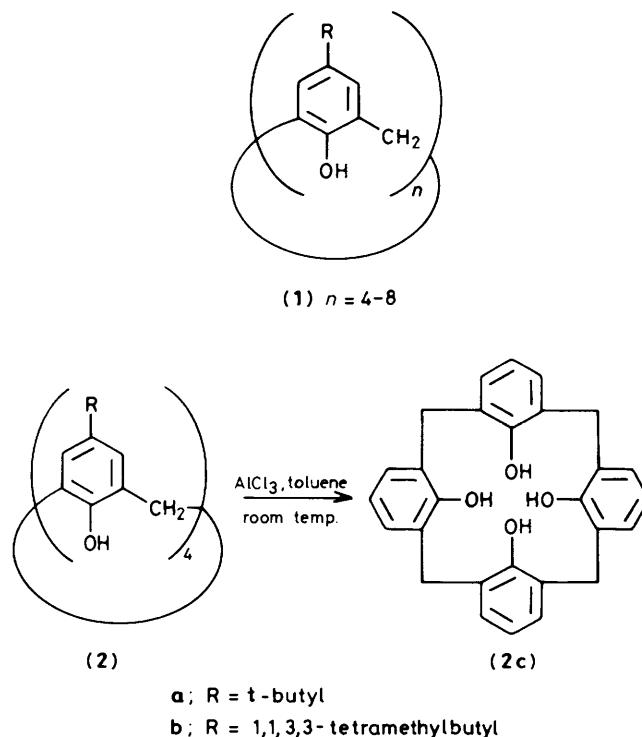
The cyclic tetramer (**2c**), formally derived from the condensation of phenol and formaldehyde but actually obtained by dealkylating *p*-*t*-butyl- and *p*-octylcalix[4]arenes, crystallizes from acetone in two crystal forms. The first one, obtained in the presence of 1,2,4,5-tetramethylbenzene, is the (**2c**)-acetone (1:1) clathrate, orthorhombic, space group *Pnma*,  $a = 17.010(8)$ ,  $b = 14.127(6)$ ,  $c = 10.667(3)$  Å,  $Z = 4$ , final  $R$  value 0.090. The second, obtained from pure acetone or in the presence of thymol, is the (**2c**)-acetone (3:1) clathrate, space group  $P6_3/m$ ,  $a = b = 14.543(5)$ ,  $c = 18.228(7)$  Å,  $\gamma = 120^\circ$ , final  $R$  value 0.070. The geometry of macrocycle (**2c**) in the two forms, in the 'cone' conformation in both cases, is slightly different. The orthorhombic crystals show a molecular arrangement of an intercalato-clathrate type and the hexagonal one a tubulato-clathrate type.

Two types of molecular inclusion compounds have so far been observed in the solid state with some calixarene hosts (**1**) which are a class of phenolic macrocycles having methylene bridges at positions *ortho* to the hydroxy groups.<sup>2</sup> The first type has been shown by complexes of *p*-*t*-butylcalix[4]arene (**2a**) and aromatic compounds of suitable size,<sup>3</sup> which have always shown an intramolecular host-guest character<sup>4</sup> with the guest held inside a molecular cavity. These compounds were the first examples of synthetic uncharged host-uncharged guest inclusion complexes, which, as the topology in the solid state<sup>3</sup> shows is a totally enclosed cage structure, can be classified as criptato-cavitate according to a recently proposed nomenclature of host-guest-type compounds.<sup>5</sup>

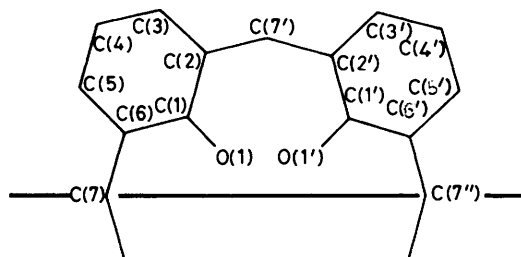
The second class of inclusion compounds, which are more of the clathrate type, although with a high degree of structural order and a 1:1 stoichiometry, has been shown by the *p*-octylcalix[4]arene (**2b**) with toluene or benzene as the guests.<sup>6</sup> Channel-type clathrates with aliphatic compounds as guests have also been shown by other calixarene macrocycles.<sup>7,8</sup> Besides the cone conformation of the calixarene molecule, which is stabilized by four intramolecular hydrogen bonds between the hydroxy groups, a special role in stabilizing the complexes of both types, between calix[4]arenes and aromatic molecules, seems to be played by the interaction between the alkyl groups *R* in the host and the aromatic rings of the guest as a result of attractive and co-operative  $\text{CH}_3-\pi$  interactions.<sup>3,6</sup> To gain more insight into this role, which could be helpful in designing new and selective host molecules, in rationalizing the factors that control the inclusion of a neutral molecule in apolar cavities, and into the clathration phenomenon in general, we studied the inclusion properties of macrocycle (**2c**) obtained from either *p*-*t*-butylcalix[4]arene (**2a**) or the *p*-octylcalix[4]arene (**2b**) by removing the *R* groups. This can be easily accomplished through an aluminium chloride-catalysed alkyl-transfer reaction,<sup>9</sup> a procedure that has already been applied successfully to calixarene substrates.<sup>8,10-12</sup> In both cases compound (**2c**) showed the same spectral and physical data recently reported by Gutsche and Levine.<sup>12</sup>

### Experimental

**Crystallization Experiments.**—Compound (**2c**) is quite soluble in both aromatic and aliphatic solvents, and is more so



than the starting compounds (**2a**) and (**2b**). On the assumption, which was justified by our previous results,<sup>3,6</sup> that  $\text{CH}_3-\pi$  interactions could give a significant contribution to the stabilization of host-guest neutral complexes, it was decided to carry out several crystallization experiments in aliphatic solvents and in the presence of equimolar quantities of aromatic compounds carrying alkyl substituents, *i.e.*, 1,2,4,5-tetramethylbenzene (durene) and thymol, which would favour their inclusion in the cavity. The results have been quite remarkable, having obtained the hexagonal phase of the acetone (3:1) clathrate in the presence of thymol and the orthorhombic (1:1) phase in the presence of durene, indicating that aromatic compounds were not included but were able to induce

**Table 1.** Calix[4]arene-acetone (1:1) clathrate. Fractional atomic co-ordinates ( $\times 10^4$ ) with standard deviations in parentheses

	x	y	z		x	y	z
O(1)	2 628(3)	3 424(4)	2 159(5)	C(3')	3 949(6)	4 967(7)	-1 191(12)
C(1)	2 138(6)	3 829(7)	1 274(10)	C(4')	4 478(6)	4 582(7)	-2 028(13)
C(2)	2 393(5)	4 621(7)	628(9)	C(5')	4 915(5)	3 796(8)	-1 683(12)
C(3)	1 876(7)	5 020(7)	-234(10)	C(6')	4 785(5)	3 395(7)	-490(11)
C(4)	1 138(7)	4 637(8)	-506(13)	C(7')	3 197(5)	5 065(6)	870(10)
C(5)	927(6)	3 821(7)	131(11)	C(7'')	5 275(6)	1/4	-63(13)
C(6)	1 415(5)	3 391(8)	995(9)	O(1ac)	2 300(9)	1/4	5 713(35)
C(7)	1 137(8)	1/4	1 736(14)	C(1ac)	2 820(8)	1/4	6 660(16)
O(1')	4 136(4)	3 438(4)	1 515(6)	C(2ac)	2 659(17)	1/4	7 955(23)
C(1')	4 245(5)	3 783(8)	395(10)	C(3ac)	3 609(9)	1/4	5 941(18)
C(2')	3 807(5)	4 597(8)	-47(12)				

**Table 2.** Calix[4]arene-acetone (1:1) clathrate. Bond distances (Å), bond angles ( $^\circ$ ), and selected torsion angles ( $^\circ$ ), with standard deviations in parentheses

## (a) Bond distances

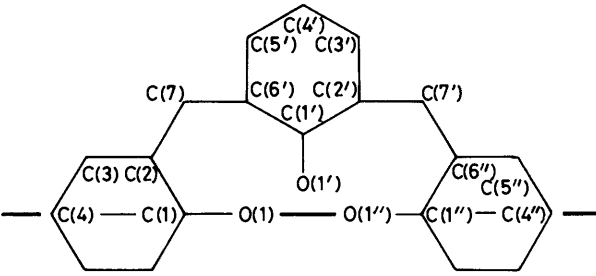
O(1)-C(1)	1.384(11)	O(1')-C(1')	1.305(12)
C(1)-C(2)	1.384(14)	C(1')-C(2')	1.449(15)
C(1)-C(6)	1.409(14)	C(1')-C(6')	1.427(14)
C(2)-C(7')	1.527(12)	C(2')-C(7')	1.572(14)
C(2)-C(3)	1.392(14)	C(2')-C(3')	1.350(17)
C(3)-C(4)	1.398(17)	C(3')-C(4')	1.380(16)
C(4)-C(5)	1.386(15)	C(4')-C(5')	1.386(14)
C(5)-C(6)	1.382(14)	C(5')-C(6')	1.411(17)
C(6)-C(7)	1.560(14)	C(6')-C(7'')	1.581(12)
O(1ac)-C(1ac)	1.34(3)		
C(1ac)-C(2ac)	1.41(3)		
C(1ac)-C(3ac)	1.55(2)		

## (b) Bond angles

O(1)-C(1)-C(6)	119.3(9)	O(1')-C(1')-C(6')	123.7(9)
O(1)-C(1)-C(2)	119.1(9)	O(1')-C(1')-C(2')	121.5(9)
C(2)-C(1)-C(6)	121.6(9)	C(2')-C(1')-C(6')	114.8(9)
C(1)-C(2)-C(7')	121.9(9)	C(1')-C(2')-C(7')	118.0(9)
C(1)-C(2)-C(3)	117.3(9)	C(1')-C(2')-C(3')	120.7(9)
C(3)-C(2)-C(7')	120.8(8)	C(3')-C(2')-C(7')	121.2(10)
C(2)-C(3)-C(4)	123.2(10)	C(2')-C(3')-C(4')	123.4(10)
C(3)-C(4)-C(5)	116.9(11)	C(3')-C(4')-C(5')	119.6(11)
C(4)-C(5)-C(6)	122.5(9)	C(4')-C(5')-C(6')	118.5(10)
C(1)-C(6)-C(5)	118.2(9)	C(1')-C(6')-C(5')	123.0(9)
C(5)-C(6)-C(7)	120.7(7)	C(5')-C(6')-C(7'')	119.9(9)
C(1)-C(6)-C(7)	120.8(7)	C(1')-C(6')-C(7'')	117.1(8)
C(6)-C(7)-C(6')	107.6(5)	C(2)-C(7')-C(2')	108.2(8)
O(1ac)-C(1ac)-C(2ac)	128(2)	C(6')-C(7'')-C(6'')	106.2(5)
O(1ac)-C(1ac)-C(3ac)	101(2)		
O(2ac)-C(1ac)-C(3ac)	131(2)		

## (c) Torsion angles

C(1)-C(2)-C(7')-C(2')	90.8(10)	C(1')-C(2')-C(7')-C(2)	-92.9(10)
C(3)-C(2)-C(7')-C(2')	-91.1(10)	C(3')-C(2')-C(7')-C(2)	90.3(11)
C(5)-C(6)-C(7)-C(6')	93.1(11)	C(5')-C(6')-C(7'')-C(6'')	-90.3(10)
C(1)-C(6)-C(7)-C(6')	-93.0(10)	C(1')-C(6')-C(7'')-C(6'')	92.1(13)

**Table 3.** Calix[4]arene-acetone (3:1) clathrate. Fractional atomic co-ordinates ( $\times 10^4$ ) with standard deviations in parentheses


	x	y	z		x	y	z
O(1)	3 866(1)	4 429(2)	1/4	C(6')	4 341(2)	3 439(3)	779(2)
C(1)	4 905(3)	4 577(3)	1/4	C(7')	4 847(3)	4 548(2)	3 905(2)
C(2)	5 388(2)	4 649(2)	1 834(2)	O(1'')	1 564(2)	1 367(3)	1/4
C(3)	6 418(2)	4 817(2)	1 845(2)	C(1'')	1 925(3)	637(4)	1/4
C(4)	6 948(3)	4 909(3)	1/4	C(4'')	2 590(4)	-821(4)	1/4
C(7)	4 847(3)	4 548(2)	1 095(2)	C(5'')	2 430(3)	-455(2)	1 831(3)
O(1')	2 836(2)	2 853(2)	1 564(1)	C(6'')	2 083(2)	292(2)	1 826(2)
C(1')	3 370(2)	2 622(3)	1 047(2)	O(1ac)	2/3	1/3	7 743(12)
C(2')	2 920(3)	1 573(3)	779(2)	C(1ac)	2/3	1/3	7 077(12)
C(3')	3 439(3)	1 376(3)	220(2)	C(2ac)	6 993(12)	2 660(12)	6 664(13)
C(4')	4 373(3)	2 173(4)	-63(2)	C(3ac)	6 536(13)	4 281(12)	6 657(14)
C(5')	4 833(3)	3 199(3)	222(2)				

**Table 4.** Calix[4]arene-acetone (3:1) clathrate. Bond distances ( $\text{\AA}$ ), bond angles ( $^\circ$ ), and selected torsion angles ( $^\circ$ ), with standard deviations in parentheses

(a) Bond distances			
C(1)-C(2)	1.380(4)	C(1')-C(6')	1.402(4)
C(1)-O(1)	1.416(6)	C(1)-C(2)	1.413(6)
C(2)-C(3)	1.392(4)	C(1)-O(1')	1.366(5)
C(2)-C(7)	1.530(5)	C(2)-C(3')	1.381(6)
C(3)-C(4)	1.391(4)	C(3)-C(4')	1.371(5)
C(7)-C(6')	1.513(5)	C(4)-C(5')	1.395(6)
C(1'')-C(6'')	1.389(5)	C(5)-C(6')	1.384(6)
C(1'')-O(1'')	1.400(8)	C(7)-C(2')	1.530(5)
C(4'')-C(5'')	1.396(6)	O(1ac)-C(1ac)	1.21(3)
C(5'')-C(6'')	1.408(6)	C(1ac)-C(2ac)	1.49(3)
C(6'')-C(7')	1.516(5)	C(1ac)-C(3ac)	1.66(3)
(b) Bond angles			
O(1)-C(1)-C(2 <sup>i</sup> )	118.4(2)	C(1')-C(6')-C(7)	121.2(3)
C(2)-C(1)-C(2 <sup>i</sup> )	123.2(3)	C(2)-C(7)-C(6'')	112.7(3)
C(2)-C(1)-O(1)	118.4(2)	O(1'')-C(1'')-C(6'')	117.8(3)
C(1)-C(2)-C(7)	123.3(3)	C(6'')-C(1'')-C(6'')	124.4(2)
C(1)-C(2)-C(3)	117.6(3)	C(5'')-C(4'')-C(5'')	121.8(3)
C(3)-C(2)-C(7)	119.1(3)	C(4'')-C(5'')-C(6'')	119.5(4)
C(2)-C(3)-C(4)	121.7(3)	C(1'')-C(6'')-C(5'')	117.4(3)
C(3)-C(4)-C(3 <sup>i</sup> )	118.3(2)	C(1)-C(2 <sup>i</sup> )-C(7 <sup>i</sup> )	123.3(3)
C(2)-C(7)-C(6')	113.0(3)	C(1'')-C(6'')-C(7 <sup>i</sup> )	123.1(3)
C(2)-C(1)-O(1')	119.4(4)	C(5'')-C(6'')-C(7 <sup>i</sup> )	119.4(3)
C(6')-C(1)-O(1')	119.2(3)	O(1ac)-C(1ac)-C(3ac)	117(2)
C(6')-C(1)-C(2')	121.4(4)	O(1ac)-C(1ac)-C(2ac)	120(2)
C(1')-C(2)-C(3')	118.2(4)	C(2ac)-C(1ac)-C(3ac)	121(2)
C(2)-C(3)-C(4')	121.0(4)		
C(3)-C(4)-C(5')	120.4(4)		
C(4)-C(5)-C(6')	120.8(4)		
C(5)-C(6)-C(7)	120.7(4)		
C(5)-C(6)-C(1')	118.1(4)		
(c) Torsion angles			
C(1)-C(2)-C(7)-C(6')	-96.1(4)	C(1')-C(2')-C(7')-C(6'')	-77.9(5)
C(3)-C(2)-C(7)-C(6')	83.6(4)	C(3')-C(2')-C(7')-C(6'')	101.3(4)
C(1'')-C(6'')-C(7')-C(2')	77.1(5)	C(1'')-C(6'')-C(7')-C(2')	96.6(4)
C(5'')-C(6'')-C(7')-C(2')	-102.0(4)	C(5'')-C(6'')-C(7')-C(2')	-82.7(4)

preferential crystal formation. This phenomenon has been observed several times and exploited with great success in chiral recognition.<sup>13</sup> At this stage we repeated the experiments with pure solvents.

Crystallization from acetone gives the orthorhombic crystals. From aromatic and chlorinated solvents we always obtained a

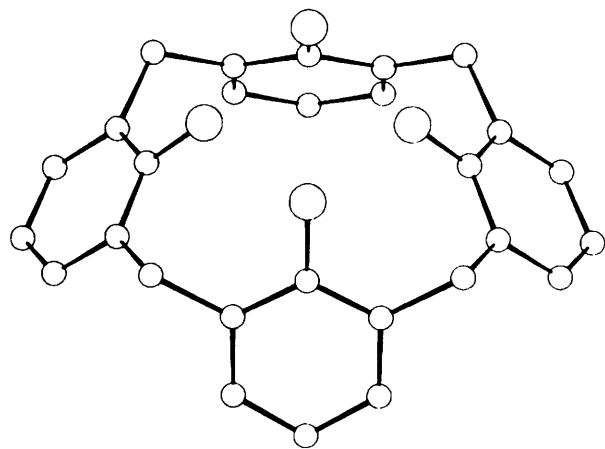


Figure 1. Perspective view of the calix[4]arene molecule

finely powdered hexagonal (empty?) phase. Crystals of the hexagonal phase are usually coloured (from pale yellow to brown). For example, from tetrachloroethylene yellow and colourless hexagonal bipyramids are obtained but the single-crystal analysis of both of them<sup>14</sup> revealed no structural differences at all. So it seems that impurities are responsible for the appearance of the colour, the morphology always being the same. In fact, if the crystals formed at the beginning are taken away from the mother liquor these are generally coloured, and the last ones are practically colourless. In this case the channel structure of the hexagonal phase could preferentially include the impurity, which is hence removed from the solvent leaving the purified phase to crystallize later.

*X-Ray Structure Analysis.*—Calix[4]arene-acetone (1:1) clathrate. The crystals were colourless prisms elongated on [001]. They rapidly faded on contact with the air and were sealed in a Lindeman capillary for the X-ray analysis. Lattice parameters were refined by least-squares fit of 29  $(\theta, \chi, \varphi)_{hkl}$  measurements taken on a Siemens AED single-crystal diffractometer on-line to a General Automation Jumbo 220 minicomputer.<sup>15</sup> A specimen of  $0.3 \times 0.3 \times 0.6$  mm was used for data collection.

*Crystal data.*  $C_{28}H_{24}O_4 \cdot C_3H_6O$ ,  $M = 424.5 + 58.0$ . Orthorhombic,  $a = 17.010(8)$ ,  $b = 14.127(6)$ ,  $c = 10.677(3)$  Å,  $U = 2566(2)$  Å<sup>3</sup>,  $Z = 4$ ,  $D_c = 1.25$  g cm<sup>-3</sup>,  $F(000) = 1024$ . Cu-K $\alpha$  radiation,  $\lambda = 1.5418$  Å,  $\mu(\text{Cu-K}\alpha) = 6.4$  cm<sup>-1</sup>.

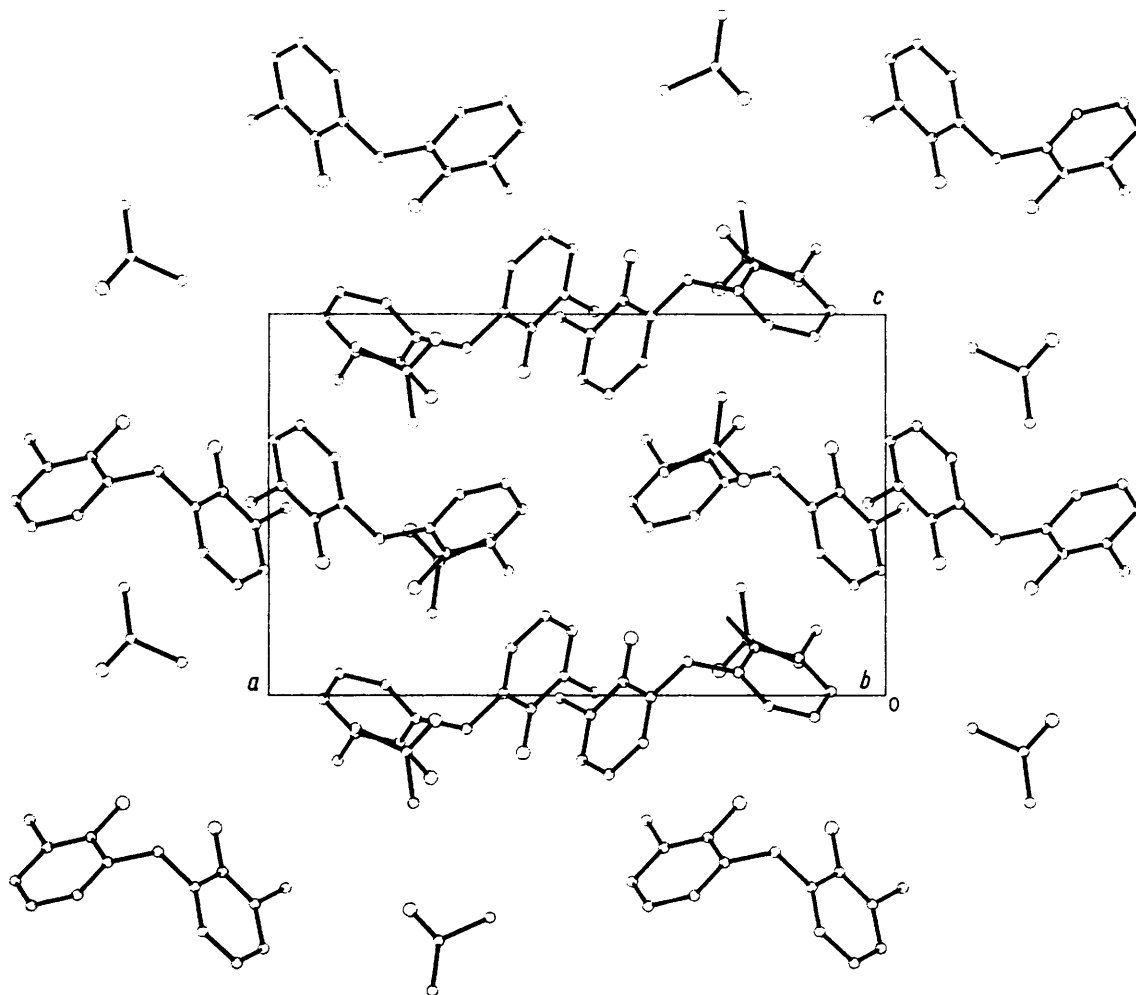


Figure 2. Molecular packing diagram along [010] of the orthorhombic phase

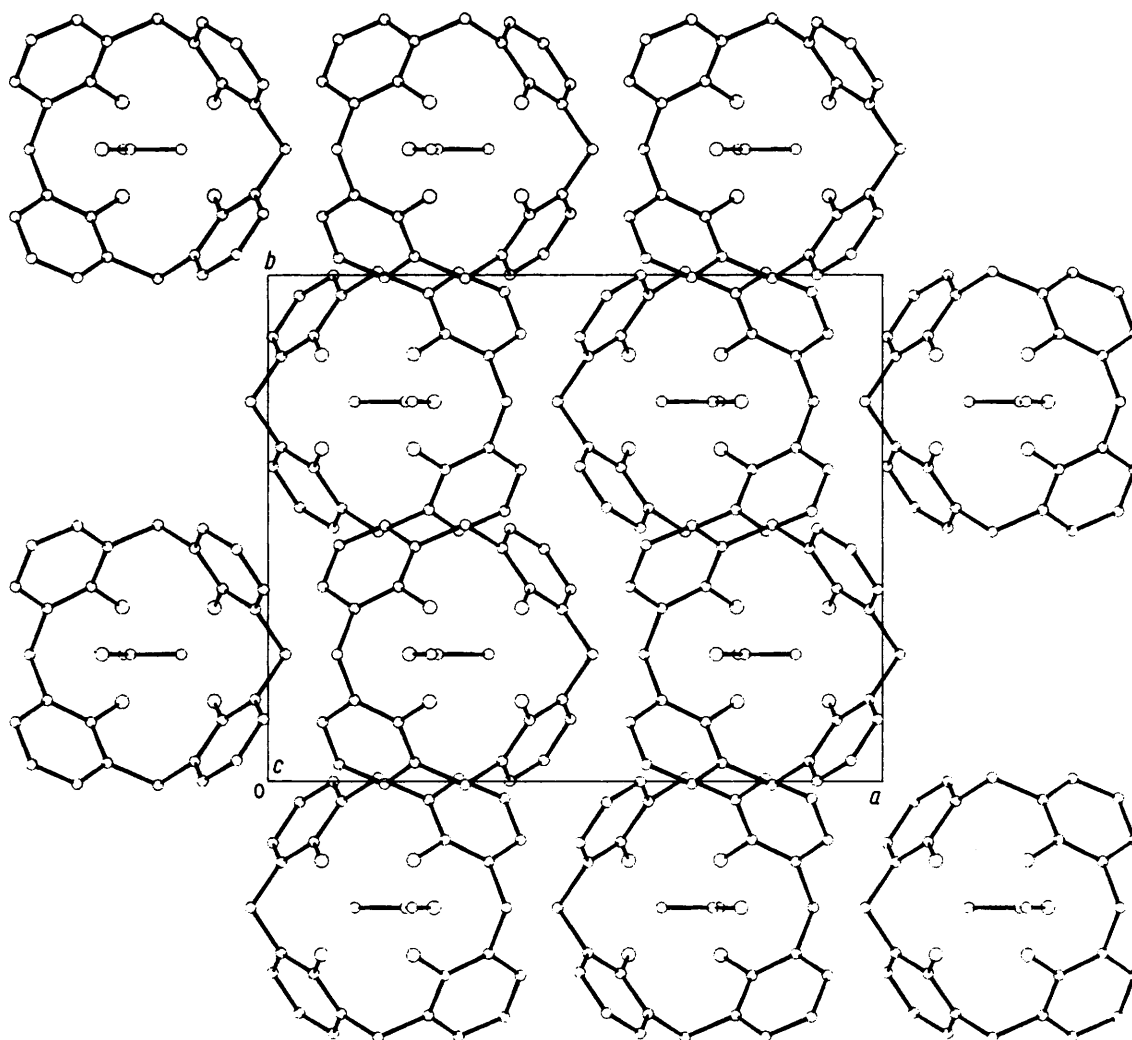


Figure 3. Molecular packing diagram along [001] of the orthorhombic phase

Absent spectra:  $0kl$   $k + l \neq 2n$ ,  $hk0$   $h \neq 2n$  define space groups  $Pnma$  or  $Pn2_1a$  ( $D_{2h}^{16}$ , No. 62 or  $C_{2v}^0$ , No. 33 setting  $a\bar{c}b$ ). Space group  $Pnma$  was chosen on the basis of the results of the analysis.

Intensity measurements were performed up to  $\theta$  70° by use of the  $\omega$ -2 $\theta$  step-scanning mode with Ni-filtered Cu- $K_\alpha$  radiation. The method described in reference 16 was used to analyse the reflection profiles. Two standard reflections recorded every hour showed a significant decay in the intensity of about 5% by the end of the data collection and so the data have been re-scaled accordingly. A total of 2 454 reflections were measured and 1 085 significant ones with  $I > 3\sigma(I)$  [ $\sigma(I)$  based on counting statistics] have been retained. No corrections were made for absorption.

**Structure analysis and refinement.** The structure was solved by direct methods using the SHELX system of programs<sup>17</sup> in the non-centrosymmetric space group. Full-matrix least-squares refinement was carried out with anisotropic thermal parameters and it stopped at  $R$  0.15 with quite a high correlation among the parameters. So it was decided to repeat the refinement process in the centrosymmetrical space group  $Pnma$ . The convergence was reached at  $R$  0.090 with unit weights and with the hydrogens in their calculated positions, with C-H = 1.08 Å. The final difference electron-density map showed the highest residual peaks of ca.  $0.4 \text{ e } \text{Å}^{-3}$ . Plots of  $|\Delta F|$  as a function of

scattering angle, magnitude of  $|F_o|$ , and Miller indices showed no particular trends. Among the last collected reflections ten, showing a large  $\Delta F$ , have been omitted from the refinement.

Scattering factors were taken from reference 18. Atomic fractional co-ordinates are listed in Table 1 and various parameters connected with the molecular geometry are given in Table 2.

**Calix[4]arene-acetone (3:1) clathrate.** Crystals are pale yellow hexagonal bipyramids with large {0001} pinacoids. They can stand in air for long periods without loss of acetone. Lattice parameters were determined by a least-squares fit of 30  $(\theta, \chi, \varphi)_{hkl}$  measurements taken on a Philips PW1100 single-crystal diffractometer equipped with a graphite monochromator. A specimen of  $0.6 \times 0.6 \times 0.4 \text{ mm}$  was used for data collection.

**Crystal data.**  $C_{28}H_{24}O_4 \cdot \frac{1}{3}C_3H_6O$ ,  $M = 424.5 + \frac{1}{3}58.0$ . Hexagonal,  $a = b = 14.543(5)$ ,  $c = 18.228(7)$  Å,  $\gamma = 120^\circ$ ,  $U = 3\ 339(2)$  Å<sup>3</sup>,  $Z = 6$ ,  $D_c = 1.32 \text{ g cm}^{-3}$ ,  $F(000) = 1\ 408$ . Mo- $K_\alpha$  radiation,  $\lambda = 0.7107$  Å,  $\mu(\text{Mo-}K_\alpha) = 0.8 \text{ cm}^{-1}$ . Absent spectra:  $000l$   $l \neq 2n$  define space groups  $P6_3$  or  $P6_3/m$  ( $C_6^0$ , No. 173 or  $C_{6h}^2$ , No. 176) and the latter was confirmed by the analysis.

Intensity data were measured up to  $\theta$  26° by use of the  $\omega$ -2 $\theta$  scan mode with Zr-filtered Mo- $K_\alpha$  radiation and with a scan rate of  $2^\circ \text{ min}^{-1}$ . Two standard reflections were recorded after each hour and they showed no significant fluctuations in

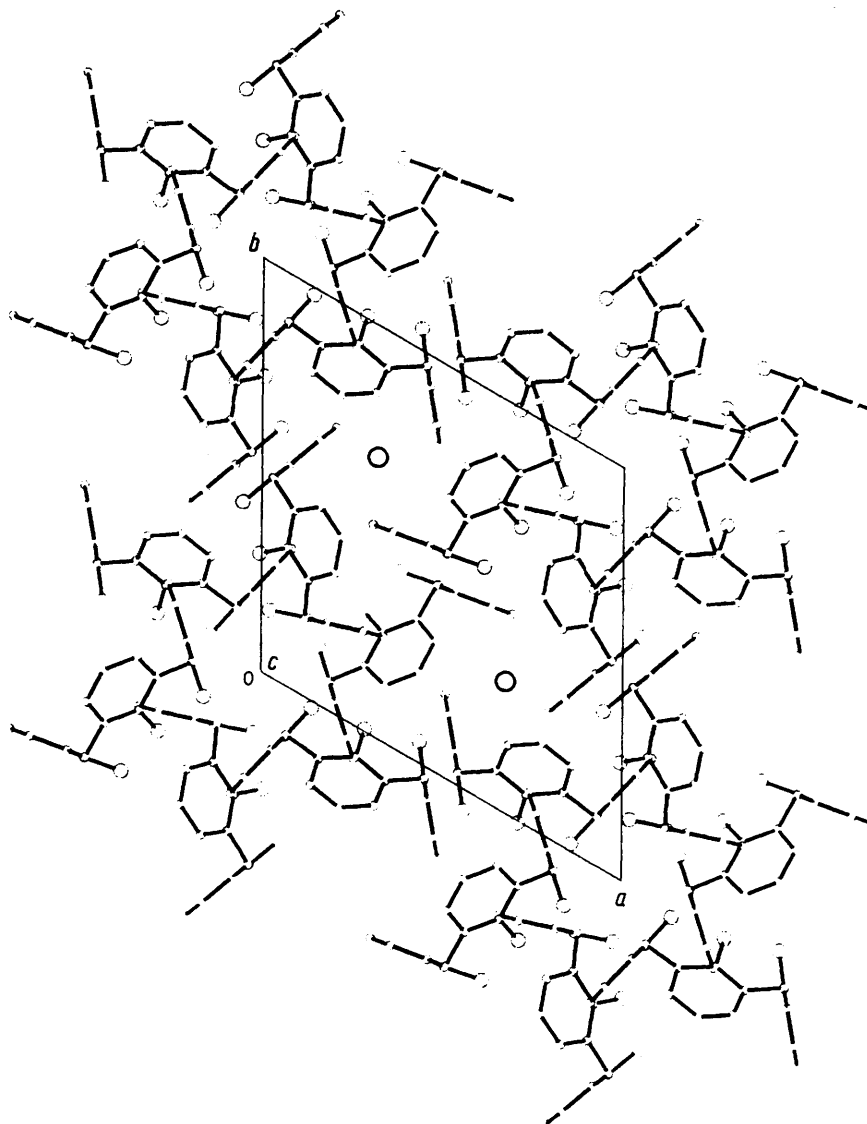


Figure 4. Molecular packing diagram along [001] of the hexagonal phase

intensity. A total of  $6\,559 \pm h,k,l$  reflections has been measured and 3 940 were used in the analysis.

**Structure analysis and refinement.** The structure was solved by direct methods and the refinement was carried out in the centrosymmetric space group  $P6_3/m$ . Full-matrix anisotropic least-squares procedures have been used. The hydrogen atoms were included in the refinement in their geometrically constructed positions with  $C-H = 1.08 \text{ \AA}$  and with variable isotropic thermal parameters. Without the contribution of the acetone molecule the refinement stopped at  $R = 0.104$ . With the inclusion of the acetone molecule with isotropic thermal parameters the refinement reached  $R = 0.070$ . The occupancy factor of the acetone molecule refined to values close to 0.9 with thermal parameters  $U = 0.10 \text{ \AA}^2$ . Several attempts have been made to locate more accurately the acetone molecule, lowering the symmetry in space groups  $P6_3$ ,  $P2_1/m$ , and  $P2_1$  but the results were not significantly different from those obtained in the space group  $P6_3/m$  that had been assigned to the crystals. The final difference electron-density map showed the highest residual peaks of  $ca. 0.3 \text{ e \AA}^{-3}$ . Plots of  $|\Delta F|$  as a function of  $\sin\theta/\lambda$ ,  $|F_o|$ , and Miller indices showed a linear

trend. Scattering factors were taken from reference 18. Atomic fractional co-ordinates are listed in Table 3 and molecular geometry parameters are reported in Table 4.

### Molecular Geometry and Discussion

The conformation of the calix[4]arene molecules observed in the two crystalline phases is significantly different. Figure 1 shows a perspective view of the molecule. The main differences concern the orientation of the phenyl rings with respect to the mean plane of the bridging methylene group [the dihedral angles formed by the aromatic rings are  $115.3(1)$ ,  $115.5(1)$ , and  $137.2(1)^\circ$  in the hexagonal phase and  $123.0(3)$  and  $125.3(3)^\circ$  in the orthorhombic]. The corresponding values in the *p*-*t*-butyl-calix[4]arene-toluene complex<sup>3</sup> are  $123(1)^\circ$  (in this compound the molecule possesses a four-fold symmetry). Hence in the hexagonal crystals two opposite rings are pushed in the direction of the calix and two are pulled, giving the molecule a more asymmetric shape. This distortion has practically no effect on the intramolecular hydrogen-bonding system, mainly responsible for the calix shape of the molecule (the  $O \cdots O$

contacts are therefore comparable in the two compounds and in the already quoted *p*-*t*-butyl derivative), but it significantly deforms the angles at the bridging methylene carbon atoms, which increase from 106.2(5), 108.2(8), and 107.6(5)° in the orthorhombic phase to 112.7(3) and 113.0(3)° in the hexagonal one [the corresponding value in the *p*-*t*-butylcalix[4]arene is 112.5(5)°]. So the significant increase in the packing forces from the orthorhombic to the hexagonal phase (the increase of the crystal density from 1.25 to 1.32 g cm<sup>-3</sup> gives a quantitative estimate of the effect) affects the conformation of the macrocycle and deforms the shape of the molecule. In both crystals the molecule loses the four-fold symmetry, but they possess a plane of symmetry which goes through the methylene carbon atoms in the orthorhombic phase and through the O—C...C lines of two *trans* phenolic groups in the hexagonal one (see the diagrams in Tables 1 and 3).

The crystal packing is shown in Figures 2 and 3 for the orthorhombic phase and in Figure 4 for the hexagonal one. The orthorhombic crystals show a molecular arrangement of an intercalato-clathrate, binary, bimolecular, mononuclear (b, 2m, 1n-intercalato-clathrate) according to the nomenclature recently proposed by Weber and Josel.<sup>5</sup> The building block of the crystal is a calix[4]arene-acetone couple with a CH<sub>3</sub> group pointing into the calix cavity.

By a translation along *c* the blocks are piled in an alternation or intercalation of acetone-calixarene-acetone molecules, forming a column parallel to [001].

Piles parallel to *b* form a layer with all the acetone-calixarene couples pointing in the same direction, *i.e.*, all the calices show the concavity in the same direction. We could define such an arrangement as a 'polar layer' with the molecular dipoles of the single building blocks being parallel.

Finally, the crystal packing is formed by an anti-parallel arrangement, along *a* of the polar layers. Contacts are consistent with van der Waals interactions.

The molecular arrangement in the hexagonal crystals is quite different. It can be classified as tubulato-clathrate, binary, hexamolecular, binuclear (b, 6m, 2n-tubulato-clathrate). The calixarene molecules face the 6<sub>3</sub> axis at the origin with the oxygen crown of the calix and the pile along [001] with contacts CH...phenyl. In such a way columns are formed possessing a 6<sub>3</sub> symmetry and with a polar interior part formed by the facing oxygen atoms of the calixarene molecules. The crystal packing is formed by repetition along *a* and *b* of these columns leaving at  $x = 2/3$ ,  $y = 1/3$ , and  $x = 1/3$ ,  $y = 2/3$  and running along *c*

apolar channels where the acetone molecules, in the case of our crystals, can be accommodated. We have also studied the crystal structure of some clathrates of this type with other guest molecules and the packing is practically unchanged. Contacts are consistent with van der Waals interactions.

The thermal parameters for both clathrates {calix[4]arene-acetone (1:1) and calix[4]arene-acetone (3:1)} have been deposited as Supplementary Publication No. SUP 56069 (34 pp.).\*

## References

- 1 C. Alfieri, E. Dradi, A. Pochini, R. Ungaro, and G. D. Andreetti, *J. Chem. Soc., Chem. Commun.*, 1983, 1075.
- 2 C. D. Gutsche, *Acc. Chem. Res.*, 1983, **16**, 161 and references cited therein.
- 3 G. D. Andreetti, R. Ungaro, and A. Pochini, *J. Chem. Soc., Chem. Commun.*, 1979, 1006; G. D. Andreetti, A. Mangia, A. Pochini, and R. Ungaro, 'Second International Symposium on Clathrate Compounds and Molecular Inclusion Phenomena, Parma, August 30—September 3, 1982,' Abstract Book, p. 42.
- 4 F. Vögtle, H. Sieger, and W. M. Müller, *Top. Curr. Chem.*, 1981, **98**, 107.
- 5 E. Weber and H.-P. Josel, *J. Inclusion Phenom.*, 1983, **1**, 79.
- 6 G. D. Andreetti, A. Pochini, and R. Ungaro, *J. Chem. Soc., Perkin Trans. 2*, 1983, 1773.
- 7 C. Rizzoli, G. D. Andreetti, R. Ungaro, and A. Pochini, *J. Mol. Struct.*, 1982, **82**, 133.
- 8 M. Coruzzi, G. D. Andreetti, V. Bocchi, A. Pochini, and R. Ungaro, *J. Chem. Soc., Perkin Trans. 2*, 1982, 1133.
- 9 M. Tashiro, *Synthesis*, 1979, 921.
- 10 H. Kämmerer, *Org. Prep. Proced. Int.*, 1978, **10**, 113.
- 11 V. Bocchi, D. Foina, A. Pochini, R. Ungaro, and G. D. Andreetti, *Tetrahedron*, 1982, **38**, 373.
- 12 C. D. Gutsche and J. A. Levine, *J. Am. Chem. Soc.*, 1982, **104**, 2652.
- 13 L. Addadi, Z. Berkovitch-Yellin, N. Domb, E. Gazi, M. Lahav, and L. Leiserowitz, *Nature (London)*, 1982, **296**, 21 and references cited therein.
- 14 G. D. Andreetti, R. Ungaro, and A. Pochini, unpublished data from our laboratory.
- 15 D. Belletti, F. Uguzzoli, A. Cantoni, and G. Pasquinelli, Internal Reports 1/79, 2/79, 3/79, 1979, Centro di Studio per la Strutturistica Diffraattometrica del C.N.R., Parma, Italy.
- 16 R. H. Blessing, P. Coppens, and P. Becker, *J. Appl. Crystallogr.*, 1974, **7**, 488.
- 17 G. Sheldrick, SHELX-76, Program for Crystal Structure Determination, University of Cambridge, 1976.
- 18 'International Tables for X-ray Crystallography,' Kynoch Press, Birmingham, 1974, vol. IV, pp. 99—101.

\* For details of the Supplementary Publication Scheme see Instructions for Authors, *J. Chem. Soc., Perkin Trans. 2*, 1983, Issue 1.